International Journal on Magnetic Particle Imaging
Vol 9, No 1, Suppl 1, Article ID 2303055, 5 Pages

Proceedings Article

Evaluation of magnetization dynamics influenced by Brownian relaxation in magnetic nanoparticles

S. Ota[a,*]· Y. Takemura[b]

[a]Department of Electrical and Electronic Engineering, Shizuoka University, Hamamatsu, Japan
[b]Department of Electrical and Computer Engineering, Yokohama National University, Yokohama, Japan
[*]Corresponding author, email: ota.s@shizuoka.ac.jp

Abstract

Magnetic relaxations determine the magnetization properties of magnetic nanoparticles for biomedical applications such as the tracer of magnetic particle imaging. In this study, the magnetization dynamics influenced by the dynamics of the particle body as the easy axes of magnetic nanoparticles of different structures were evaluated measuring the magnetization curves, intensity of harmonic components in magnetization, and oscillation and orientation of the easy axis. To observe the effects of the Brownian relaxation associated with particle rotation, we prepared magnetic nanoparticles fixed with epoxy resin to inhibit the particle rotation and dispersed them in water where the particle rotation occurred. It is indicated that the Brownian relaxation observed as the particle oscillation and orientation significantly affected the magnetization dynamics of magnetic nanoparticles in the ferromagnetic regime.

I. Introduction

Magnetic relaxation is the most characteristic phenomenon of magnetic nanoparticles (MNPs), which are used in biomedical applications such as tracers of magnetic particle imaging (MPI) [1]. Magnetic relaxations are conventionally divided into the Néel relaxation, derived from the rotation of magnetic moments, and the Brownian relaxation, associated with the physical rotation of MNPs under an applied magnetic field. The harmonic signal derived from the nonlinear magnetization response is characterized by MPI. Based on the fact that the Brownian relaxation time depended on viscosity, the viscosity mapping technique was developed as an application of color MPI [2]. Intracranial cerebral hemorrhage was monitored by distinguishing the MPI signals of liquid blood from coagulated blood where MNPs were injected [3].

Models of magnetic relaxation, as typified by the egg model by Shliomis and Stepanov, were theoretically constructed [4]. The time-dependent dynamics of the magnetic moment and particle body are respectively determined by the Néel and Brownian relaxation times τ_N and τ_B given by

$$\tau_\mathrm{N} = \tau_0 \exp\left(\frac{K V_\mathrm{M}}{k_\mathrm{B} T}\right), \tag{1}$$

$$\tau_\mathrm{B} = \frac{3\eta V_\mathrm{H}}{k_\mathrm{B} T}, \tag{2}$$

where τ_0, K_u, V_M, k_B, T, η, and V_H denote the attempt time, anisotropy constant, core volume of the MNPs, Boltzmann constant, temperature, viscosity of the solvent, and hydrodynamic volume of the MNPs, respectively. Generally, Néel and Brownian relaxations occur in parallel, as illustrated by the effective relaxation time $\tau_{eff} = \tau_N \tau_B / (\tau_N + \tau_B)$ [5]. We observed that Brownian relaxation occurred after Néel relaxation by applying a pulsed magnetic field [6]. We also observed the contribution of the Brownian relaxation under an alternating current (AC) magnetic field [7]. Based on these theoretical considerations, the dependence of the Néel [8] and Brownian [9] relaxation times on the applied field strength were clarified. Both the Néel and Brownian relaxation times decreased as the applied field strength increased. Furthermore, the increase in the effective anisotropy constant improved the magnetic torque, which induced the rotation of the easy axis [10]. In addition, measurements [6] and numerical simulations [11] showed that the Néel relaxation time was affected by the dipole interaction.

In this study, the magnetization dynamics represented by the complex relaxation model as the superimposition of the Néel and Brownian relaxations with respect to MNPs dispersed in a liquid were empirically investigated. The influence of the Brownian relaxation on the Nèel relaxation was discussed based on the rotation of the magnetic moments and particle bodies. The frequency dependence of the harmonic components of magnetization under an AC magnetic field was measured over a frequency range of 200 Hz–200 kHz. The oscillation and orientation of the particle bodies under an AC magnetic field were also measured by observing the permeation of light entering the magnetic fluid [12]. Investigation of the magnetization dynamics of MNPs dispersed in solids and liquids is important for characterizing the imaging of solid objects, such as tumors and organs, and liquids such as blood [13].

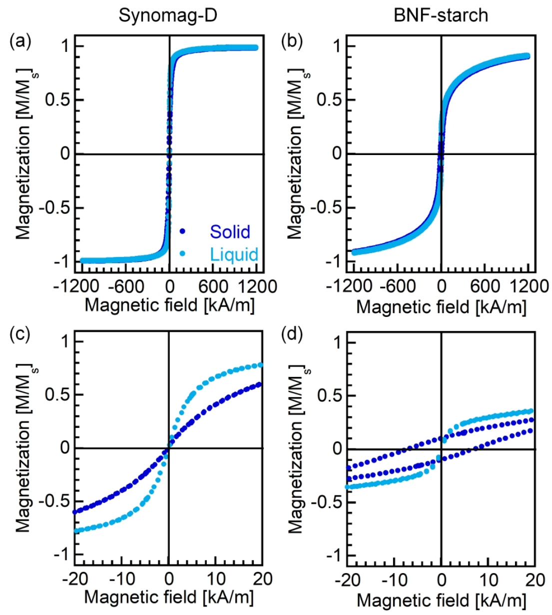

Figure 1: Magnetization curves under DC magnetic field of 0-1200 kA/m in (a) Synomag®-D, and (b) BNF-starch. The magnified graphs around the origin in (a) and (b) were shown in (c) and (d), respectively.

II. Material and methods

II.I. Sample preparation

Iron oxide nanoparticles of different particle structures, such as the multicore in Synomag®-D and cubic shape in BNF-starch purchased from Micromod Partikeltechnologie GmbH (Rostock, Germany), were measured. These nanoparticles were fixed with epoxy resin and dispersed in diluted water as solid and liquid samples, respectively.

II.II. Measurement method

Magnetization curves were obtained using a vibrating sample magnetometer (VSM) under direct-current (DC) magnetic fields of 0–1200 kA/m. The magnetization responses under an AC magnetic field were measured at an amplitude of 8 kA/m and a frequency of 200 Hz–200 kHz. The AC magnetic field was applied using an air-cooled excitation coil with 120 turns. The magnetization flux was measured using a detection coil of 100 turns at 200 Hz–10 kHz and 1 turn at 10 kHz–200 kHz. The harmonic components of the magnetization were evaluated by Fourier transformation of the measured magnetization signals under an AC magnetic field. To measure the DC magnetization curves and harmonic components, the concentration of MNPs was adjusted to 2.8 mg-Fe/mL.

The dynamics of particle bodies as the easy axis derived from magnetization dynamics under an AC magnetic field with an amplitude of 8 kA/m and a frequency of 10 Hz–100 kHz was observed by measuring the degree of optical transmission [12]. A Helmholtz-type excitation coil with 152 turns was used to apply an AC magnetic field. To measure the dynamics of the easy axis, the concentration of MNPs was adjusted to 0.2 mg-Fe/mL.

III. Results and discussion

III.I. DC magnetization curves

Figure 1 shows the DC magnetization curves in solid and liquid. The magnetization was normalized by the saturation magnetization M_s (M/M$_s$). Under experimental conditions at room temperature, Synomag®-D showed a superparamagnetic regime because of its marginal coercivity, whereas BNF-starch showed a ferromagnetic regime, as a coercivity of 6.92 kA/m was clearly observed in the solid. On the other hand, with respect to both Synomag®-D and BNF-starch, the coercivities in the liquid samples were also marginal because of the superparamagnetic behavior caused by the rotation of the easy axis of the MNPs.

When uniaxial anisotropy was represented by an MNP, the particle body corresponded to the easy axis. Because

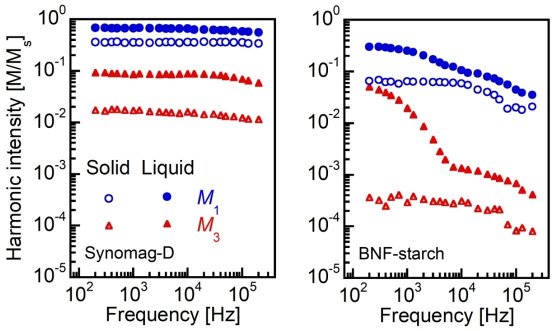

Figure 2: Frequency dependence of the fundamental and third harmonic intensity of magnetization under AC magnetic fields of 8 kA/m.

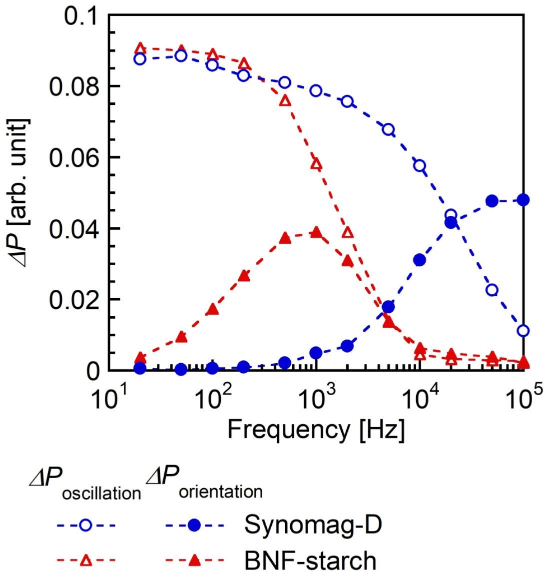

Figure 3: Frequency dependence of the oscillation and orientation of the easy axis under AC magnetic fields of 8 kA/m. $\Delta P_{\mathrm{oscillation}}$ and $\Delta P_{\mathrm{orientation}}$ are the degree of the oscillation and orientation of the easy axis evaluated by the optical transmission, respectively.

the rotation of the particle body decreased the anisotropy energy, superparamagnetic behavior was observed in the fluid [14]. With respect to Synomag®-D, the magnetization in the solid was smaller than that in the liquid under the small magnetic field strength, which illustrates that the magnetization bound to the easy axis by the small anisotropy described as the marginal coercivity [15]. It is indicated that the effective anisotropy in the clustered spherical particles was significantly smaller compared to that in the cubic particles. On the other hand, it was found that the effective anisotropy constant in the cubic particles was smaller than that in the spherical particles [16],

III.II. Harmonic intensity and easy axis dynamics

Figure 2 shows the frequency dependence of the fundamental and third-harmonic components of the magnetization under AC magnetic fields. In the solid, the signal intensities decreased with an increase in the applied field frequency because the nonlinearity of the magnetization disappeared with a reduction in the amplitude of the magnetization. With respect to Synomag®-D, a reduction in the fundamental component of magnetization was observed at a higher frequency than that in BNF-starch. This indicates that the Néel relaxation time associated with the anisotropy energy in Synomag®-D is significantly shorter than that in BNF-starch because of the small anisotropy constant with respect to multicore structure, which corresponds to the marginal coercivity in Synomag®-D and the relatively large coercivity in BNF-starch, as shown in Fig. 1(c and d).

In the liquid samples, the fundamental component was decreased at a lower frequency compared to that in the solid samples because the magnetization derived from Brownian relaxation in the liquid was inhibited, whereas only Néel relaxation occurred in the solid samples. The inflection points were observed in the third harmonic component only in the liquid samples, which was also shown in Ref. [17]. The inflection points were not observed in the fundamental component of either solid or liquid. These inflection points indicate the superimposition of the magnetic relaxations of different relaxation times derived from the Néel and Brownian relaxations. The first and second reductions of the third-harmonic components were associated with the reduced magnetization derived from the Brownian and Néel relaxations, respectively.

The oscillation and orientation of the particle body under an AC magnetic field are shown in Fig. 3, which were evaluated from the variation of the permeation intensity, ΔP. The particle body, as the easy axis of an MNP, also oscillated under an AC magnetic field. The oscillation amplitude of the easy axis $\Delta P_{\mathrm{oscillation}}$ was calculated by the minimum of ΔP subtracted from the maximum. The orientation degree $\Delta P_{\mathrm{orientation}}$ of the easy axis was assessed as ΔP where an applied magnetic field strength was zero.

When $\Delta P_{\mathrm{oscillation}}$ decreased, $\Delta P_{\mathrm{orientation}}$ increased with the applied field frequency, which indicates that the easy axis was gradually oriented toward the direction of the applied magnetic field [18,19]. The stationary orientation of the easy axis increased the phase delay of the magnetization from the applied magnetic field, which increased the imaginary part of the susceptibility [20]. When the frequency of the applied magnetic field was significantly higher than the Néel relaxation time, both the oscillation and the orientation of the easy axis associ-

10.18416/ijmpi.2023.2303055

ated with the Brownian relaxation were inhibited [21], as observed with respect to BNF-starch. This is because the rotation of the easy axis was inhibited in reducing magnetization. As both the Néel and Brownian relaxation times were shorter than the applied field frequency, a decrease in $\Delta P_{\mathrm{orientation}}$ in synomag®-D was not observed in the measured frequency range.

IV. Conclusions

This study measured commercially dispersed MNPs to evaluate the magnetic relaxation influenced by the structure of MNPs. The multicore and cubic single-core structures were demonstrated as superparamagnetic and ferromagnetic regimes, respectively, which were clarified by the DC magnetization curves in the solid samples. Furthermore, we experimentally observed the frequency dependence of the nonlinear response of the magnetization and the easy axis dynamics. When MNPs were dispersed in a liquid, the particle body, as the easy axis of an MNP, oscillated and was oriented under an AC magnetic field. The stationary orientation of the easy axis effectively enhanced the anisotropy energy, which prolonged the Néel relaxation time. When the rotation of the easy axis was inhibited, the intensity of the harmonic signal monotonically decreased as the applied field frequency increased. Conversely, the observation made at the inflection point showed that the harmonic signal depended on the frequency owing to the prolonged Néel relaxation time. This indicated that the Néel relaxation was affected by the Brownian relaxation. Considering the frequency dependence of the harmonic signal intensity was determined by the relaxation time, understanding the influence of particle structure on magnetic relaxation can contribute to the development of material design for MPI.

Acknowledgments

This work was partially supported by JSPS KAKENHI grant numbers 20H02163 and 20H05652.

Author's statement

Conflict of interest: Authors state no conflict of interest. Informed consent: Informed consent has been obtained from all individuals included in this study. Ethical approval: The research related to human use complies with all the relevant national regulations, institutional policies and was performed in accordance with the tenets of the Helsinki Declaration, and has been approved by the authors' institutional review board or equivalent committee.

References

[1] B. Gleich, J. Weizenecker, Tomographic Imaging Using the Nonlinear Response of Magnetic Particles. Nature, vol. 435, pp. 1214—1217, 20 05.

[2] M. Utkur, Y. Muslu, E. U. Saritas, Relaxation-based color magnetic particle imaging for viscosity mapping, *Appl. Phys. Lett.*, vol. 115, 152403, 2019.

[3] P. Szwargulski, M. Wilmes, E. Javidi, F. Thieben, M. Graeser, M. Koch, C. Gruettner, G. Adam, C. Gerloff, T. Magnus, T. Knopp, P. Ludewig,, Monitoring Intracranial Cerebral Hemorrhage Using Multicontrast Real-Time Magnetic Particle Imaging, *ACS Nano*, vol. 14, pp. 13913–13923, 2020.

[4] M. I. Shliomis, V. I. Stepanov, Theory of the Dynamic Susceptibility of Magnetic Fluids, Adv. Chem. Phys., vol. 87, 1993.

[5] R. Kötitz, W. Weitschies, L. Trahms, W. Brewer, W. Semmler, Determination of the Binding Reaction Between Avidin and Biotin by Relaxation Measurements of Magnetic Nanoparticles, *J. Magn. Magn. Mater.*, vol. 194, pp. 62–68, 1999.

[6] S. Ota, Y. Takemura, Characterization of Néel and Brownian relaxations isolated from complex dynamics influenced by dipole interactions in magnetic nanoparticles, *J. Phys. Chem. C*, vol. 123, pp. 28859—28866, 2019.

[7] S. Ota, T. Yamada, Y. Takemura, Dipole-dipole interaction and its concentration dependence of magnetic fluid evaluated by alternating current hysteresis measurement, *J. Appl. Phys.*, vol. 117, 17D713, 2015.

[8] W. T. Coffey, Y. P. Kalmykov, Thermal fluctuations of magnetic nanoparticles: Fifty years after Brown, *J. Appl. Phys.*, vol. 112, 121301, 2012.

[9] T. Yoshida, K. Enpuku, Simulation and Quantitative Clarification of AC Susceptibility of Magnetic Fluid in Nonlinear Brownian Relaxation Region, *Jpn. J. Appl. Phys.*, vol. 48, 127002, 2009.

[10] J. Carrey, N. Hallali, Torque undergone by assemblies of single-domain magnetic nanoparticles submitted to a rotating magnetic field, *Phys. Rev. B*, vol.. 94, 184420, 2016.

[11] P. Ilg, Equilibrium Magnetization and Magnetization Relaxation of Multicore Magnetic Nanoparticles, *Phys. Rev. B*, vol. 95, 214427, 2017.

[12] M. Suwa, A. Uotani, S. Tsukahara, Magnetic and viscous modes for physical rotation of magnetic nanoparticles in liquid under oscillating magnetic field, *J. Appl. Phys.*, vol. 125, 123901, 2019.

[13] S. Ota, R. Takeda, T. Yamada, I. Kato, S. Nohara, Y. Takemura, Effect of particle size and structure on harmonic intensity of blood-pooling multi-core magnetic nanoparticles for magnetic particle imaging, *Int. J. Magn. Part. Imag.* vol. 3, 1703003, 2017.

[14] S. Ota, Y. Takemura, Dynamics of Magnetization and Easy Axis of Individual Ferromagnetic Nanoparticle Subject to Anisotropy and Thermal Fluctuations, *J. Magn. Soc. Jpn.*, vol. 43, pp. 34–41, 2019.

[15] S. Ota, S. B. Trisnanto, S. Takeuchi, J. Wu, Y. Cheng, Y. Takemura, Quantitation method of loss powers using commercial magnetic nanoparticles based on superparamagnetic behavior influenced by anisotropy for hyperthermia, *J. Magn. Magn. Mater.*, vol. 538, 168313, 2021.

[16] H. Mamiya, H. Fukumoto, J. L. C. Huaman, K. Suzuki, H. Miyamura, J. Balachandran, Estimation of Magnetic Anisotropy of Individual Magnetite Nanoparticles for Magnetic Hyperthermia, *ACS Nano*, vol. 14, pp. 8421—8432, 2020.

[17] A. L. Elrefai, T. Yoshida, K. Enpuku, Viscosity dependent amplitude and phase of harmonic signals of magnetic nanoparticles, *J. Magn. Magn. Mater.*, vol. 507, 166809, 2020.

[18] T. Yoshida, S. Bai, A. Hirokawa, K. Tanabe, K. Enpuku, Effect of viscosity on harmonic signals from magnetic fluid, *J. Magn. Magn. Mater.*, vol. 380, pp. 105–110, 2015.

10.18416/ijmpi.2023.2303055

[19] S. Ota, Y. Takemura, Evaluation of Easy-Axis Dynamics in a Magnetic Fluid by Measurement and Analysis of the Magnetization Curve in an Alternating Magnetic Field, *Appl. Phys. Express*, vol. 10, 085001, 2017.

[20] G. Shi, R. Takeda, S. B. Trisnanto, T. Yamada, S. Ota, Y. Takemura, Enhanced specific loss power from Resovist® achieved by aligning magnetic easy axes of nanoparticles for hyperthermia, *J. Magn. Magn. Mater.*, vol. 473, 148–154, 2019.

[21] S. Ota, S. Ohkawara, H. Hirano, M. Futagawa, Y. Takemura, Empirical and simulated evaluations of easy-axis dynamics of magnetic nanoparticles based on their magnetization response in alternating magnetic field, *J. Magn. Magn. Mater.*, vol. 539, 168354, 2021.

10.18416/ijmpi.2023.2303055